Optically levitated nanosphere with high trapping frequency

YuanBin Jin, XuDong Yu and Jing Zhang

Articles you may be interested in

Effect of high temperature annealing on the performance of MANOS charge trapping memory
SCIENCE CHINA Technological Sciences **55**, 888 (2012);

Ab initio simulation of the sum-frequency generation response of optically active liquids in the presence of a dc electric field—determination of the absolute molecular configuration
SCIENCE CHINA Chemistry **57**, 1405 (2014);

Nanobowl optical concentrator for efficient light trapping and high-performance organic photovoltaics
Science Bulletin **60**, 109 (2015);

Paramagnetic Meissner effect in high T_c superconductors (I) --Flux trapping in small particles and typical behavior of paramagnetic moments
Science in China Series A-Mathematics **41**, 647 (1998);

HIGH FREQUENCY PHOTOACOUSTIC MEASUREMENTS IN AIR
Science in China Series A-Mathematics, Physics, Astronomy & Technological Science **34**, 1273 (1991);

Optically levitated nanosphere with high trapping frequency

YuanBin Jin[1,2], XuDong Yu[1,2*], and Jing Zhang[1*]

[1]*The State Key Laboratory of Quantum Optics and Quantum Optics Devices, Institute of Opto-Electronics, Shanxi University, Taiyuan 030006, China;*
[2]*Synergetic Innovation Center of Quantum Information and Quantum Physics, Shanxi University, Taiyuan 030006, China*

The optically levitated object is intrinsically isolated from the thermal bath compared with the opto-mechanical oscillator connected to the thermal environment via the cantilever [1,2]. Thus the limitation of the thermalization and decoherence introduced by the cantilever is cancelled. The *Q*-factor of the system is predicted to approach 10^{12} and the system is extremely sensitive to some changes [3-6]. And it is expected to detect non-Newtonian gravity forces at very small scales [7], the impact of single air molecules [8], nanoscale temperature [9], and magnetic spin resonance [10]. Importantly it can be used to test the fundamental physical problems. If the nanoparticle in ultra-high vacuum is cooled down to the quantum ground state, it can produce the quantum macroscopic superposition state and test the decoherence mechanism [5,11-13].

In this paper, we present the experimental study of the levitated single nanosphere using the optical trap. The high oscillation frequency of 616.7 kHz is obtained via a high-numerical-aperture (NA) objective when the power of the trapping laser is about 200 mW. The displacement of the nanosphere is measured using three pairs of position-sensitive detection systems for measuring the *x*, *y*, *z* dimensions. Using the information of the position, the center-of-mass motion trajectory is plotted. The experiment provides a platform for the further studies of the center-of-mass motion detection and cooling with the squeezed optical field.

Currently, the generation of the quantum ground state for the optically trapping mechanical system is a great challenge. Under the ultrahigh vacuum environment, the center-of-mass motion must be cooled down and almost close to the nano-Kelvin regime [3]. Several groups have reported progress in micro- and nano-scale particle trapping and cooling [2, 3, 14-16]. And significant improvement has been made, for instance, the trapping time in low vacuum can reach the magnitude of days [14], the center-of-mass motion temperature is cooled down to mili-Kevin [2] and recently 450 micro-Kelvin was achieved using the coherent feedback [16]. However further cooling of the temperature meets the obstacle because of many limitations imposed on the system, such as the vacuum degree, the lifetime, and the performance of the feedback control loop, and so on.

Herein, the particle size is a critical parameter. A larger particle has lower oscillation frequency and can make the system more stable considering the kicks of the dust and the push of the airflow. However a large particle can also cause the large recoil heating, thus a smaller particle is preferred. But a smaller particle is easily affected by air currents and dust making the system relatively unstable. To balance these concerns, particle sizes in the range of several tens of nanometers to several micrometer are usually chosen in the experiments and the particle with radius around 100 nm is predicted possessing the largest signal to noise ratio for detecting the decoherence mechanism induced by the gravitation [11]. Besides the vacuum degree, the prime limit on cooling the particle is the laser noise, i.e., the classical noise at the low frequency range and the shot noise of the laser. Previously, the trap-

*Corresponding authors (XuDong Yu, email: jiance_yu@sxu.edu.cn; Jing Zhang, email: jzhang74@yahoo.com)

ping frequency for the particle in the most experiments has been around several hundred kilo-Hz. In this range, however, most commercial solid-state lasers have large noise originating from the electronic noise and the relaxation oscillation noise. These noises can cause heating and submerge the signal when the center-of-mass motion temperature is lower than milli-Kelvin. Finally, in the detection system, the common mode rejection ratio (CMRR) and the noise floor of the detectors can also limit the signal to noise ratio. In view of the above discussions, the silica sphere with radius around 100 nm is chosen for our experiment. The trapping frequency is located far from the low frequency range, which will be extremely important when using a squeezed light field to detect and cool the particle motion in our future experimental studies. In our detection system, the current-subtraction detectors are utilized to increase CMRR and the transimpedance amplifier has a very low input current noise which reduces the noise floor.

The schematic diagram of the experiment is shown in Figure 1. The 532 nm light with TEM00 Gaussian mode is supplied by a diode-pumped intra-cavity frequency-doubled single-frequency laser and passes through an objective with NA=0.95. The objective's working distance is 0.3 mm. The strongly focused beam is collimated by a second lens with a focal length of 20 mm. The waist diameter of the trapping beam is about 0.5 μm. The lenses are placed in a vacuum chamber. And the light output from the vacuum chamber is divided into three parts for detecting the three-dimensional position information of the particle. In the detection scheme, the information of the transverse position x and y can be obtained using the D-shaped reflective mirrors, which split the laser beam into two parts. The two beams are collected by

the pair of photodiodes of a current-subtraction detector. When the nanosphere position deviates slightly from the equilibrium position in the transverse direction, the light intensities collected by the two photodiodes differ slightly and the intensity difference is proportional to the transverse displacement. The third part of the output beam is separated by a normal beams splitter in two, wherein one of the split beam is entirely collected by the photodiode and the other is partially detected after passing through a focal lens. Change in the axial position of the nanosphere will make the focus position at the z detection stage move slightly and modify the light intensity detected by the photodiode. Thus the displacement of the nanosphere in the longitudinal direction can be measured. The current subtraction is employed in the detectors, which offers a higher CMRR and better capacity before saturation when compared with single detectors. The measured CMRR value is larger than 60 dB@1 MHz. The transimpedance amplifier has a very low input current noise of about 2.3 pA/$\sqrt{\text{Hz}}$@1 MHz. The current-voltage conversion gains are 10^4, 3.3×10^3, 3.3×10^3 for the x, y, z detectors, respectively. To load the nanosphere into the device, the commercial hydrosoluble silica nanospheres are first dissolved in deionized water followed by 15 min sonication. Next the suspension is diluted and poured into an ultrasonic nebulizer. Finally the droplets containing the nanospheres are dispersed into the vacuum chamber. Once a particle is trapped, a vacuum pump is engaged to evacuate the chamber.

In theory, a dielectric sphere in the focused laser field would tackle the directional-propagation photon and then emit a photon. The scattering photons propagate in an irregular manner. Thus the sphere obtains the directional momentum which is known as the scattering force. This force can push the particle out of the trapping zone. Simultaneously, the particle also feels the gradient force which is the conservative force and related to the gradient of the trapping field. If the gradient force is sufficiently larger than the scattering force, the sphere can be trapped stably in the optical potential well. If the sphere size is much smaller than the wavelength of the trapping laser ($r \ll \lambda$, r is the radius of the sphere and λ is the wavelength of the trapping laser), i.e., the Rayleigh approximation holds [17], the sphere can be seen as a point dipole. In the present experiment, the radius $r \approx 100$ nm and the wavelength of the trapping laser $\lambda = 532$ nm, the sphere size is relatively large ($r \sim \lambda$). This corresponds to the Mie scattering and in this regime the general Lorentz-Mie theory (GLMT) has been applied extensively to analyze the sphere-medium scattering. Harada and Asakura presented a detailed comparison of the Rayleigh approximation and GLMT predictions for the transverse and longitudinal trapping forces in ref. [18]. According to our experimental datum ($r \approx$ 100 nm, $\lambda = 532$ nm, $P = 200$ mW, $NA = 0.95$), in the transverse direction, the Rayleigh scattering approximation and the GLMT almost are nearly equivalent and the trans-
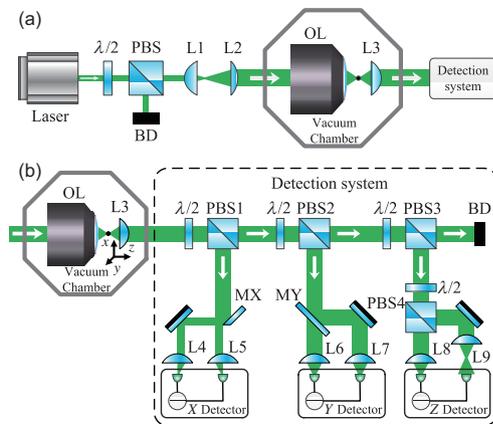

Figure 1 (Color online) Schematic diagram of the experimental setup. (a) Laser trapping system via a high-numerical-aperture objective. (b) Three pairs of position-sensitive detection systems for measuring the motion in x, y, z directions. PBS1-4, polarized beam splitter; $\lambda/2$, half-wave plate; L1-9, lens; OL, objective lens; BD, beam dump; MX and MY are D-shaped reflective mirrors that split the laser beam into two parts horizontally and vertically. x, y, and z detectors are the current-subtraction detectors with very low noise and high CMRR.

verse trapping force depends linearly on the displacement of the sphere near the equilibrium position. In the longitudinal direction, the Rayleigh-scattering approximation is not effective when considering the high-order components of the electric and magnetic fields. The GLMT can provide a relatively accurate result in this regime, in which the equilibrium position in the axial direction is pushed off the waist position of the trapping field, but the relationship between the longitudinal trapping force and the displacement near the equilibrium position is also linear. Therefore this system can be treated as a simple harmonic oscillator.

Without the feedback, the equation for the simple harmonic motion of a trapped nanosphere in a potential field in any direction x is governed by the following equation:

$$\ddot{x}(t) + \gamma \dot{x}(t) + \omega_0^2 x(t) = \frac{F_c}{m_p}, \qquad (1)$$

where $\omega_0 = \sqrt{k_x/m_p}$ is the natural angular frequency of the trapped nanosphere (k_x is the trapping stiffness, and m_p is the mass of the nanosphere). γ is the damping rate and F_c is the stochastic term that originates from the the perturbations caused by the thermal motion of air molecules, which introduces the Langevin noise and the damping.

By solving the above motion equation, we can get the noise spectrum at the analysis frequency Ω

$$S_x(\Omega) = \frac{k_B T}{m_p} \frac{\gamma}{(\omega_0^2 - \Omega^2)^2 + \Omega^2 \gamma^2}, \qquad (2)$$

where k_B is the Boltzmann constant and T is absolute temperature. Figure 2 shows the measured noise power spectra at 6.8 kPa. The discrete points represent the experimental data and the lines are the theoretical fitting. The blue, black, and red traces correspond to the x, y, and z dimensions, respectively. Herein, the power of the trapping beam is 200 mW and the beam is slightly asymmetric in the transverse direction. The measured trapping angular frequencies are $\omega_x = 2\pi \times 558.2$ kHz and $\omega_y = 2\pi \times 616.7$ kHz. The axial trapping angular frequency is $\omega_z = 2\pi \times 223.6$ kHz. By fitting the noise spectra, the damping rates $\gamma_{x,y,z} = 2\pi \times (41.7, 47.3, 46.9)$ kHz at 6.8 kPa are obtained in the x, y, z directions, respectively. Hence the Q-factors in the three dimensions are 13.4, 13.0, 4.8, respectively. But these measured Q-factors are small and the trapped particles are easy to lose in our experiment when we increase the vacuum because, besides the dust' kicks and the airflow thrust discussed above, the power stability of the trapping laser and the mechanical vibration of the optical table also limit our experiment. The damping rate according to the fluctuation-dissipation theory is as follows:

$$\gamma = \frac{6\pi \xi r}{m_p} \frac{0.619}{0.619 + \bar{\lambda}/r}(1 + c_k), \qquad (3)$$

where $\bar{\lambda}$ is the average free path of the air molecules, that is inversely proportional to the air pressure $p \cdot c_k = \frac{0.31(\bar{\lambda}/r)}{(0.785 + 1.152(\bar{\lambda}/r) + (\bar{\lambda}/r)^2)}$ and ξ is the viscosity coefficient of the air. Thus, the particle radius is $r = 93.8$ nm; consequently, the mass is $m_p = 6.91 \times 10^{-18}$ kg, according to the density of the nanosphere. The coefficients between the displacement and the signal voltage are 155 mV/nm, 5.56 mV/nm, 0.287 mV/nm for the x, y, z position detectors in our experiment, which are obtained by fitting the noise spectra. In addition, the crosstalk between the three dimensions is inevitable. But it can be minimized by adjusting the directions of the straight edge of the D mirrors in the transverse dimensions and the beam part collected by the photodiode in the longitudinal dimension. Figure 3(a) plots the noise spectra of the z dimension vs. the air pressure (the discrete points are the experimental data and the solid lines are the theoretical fitting;
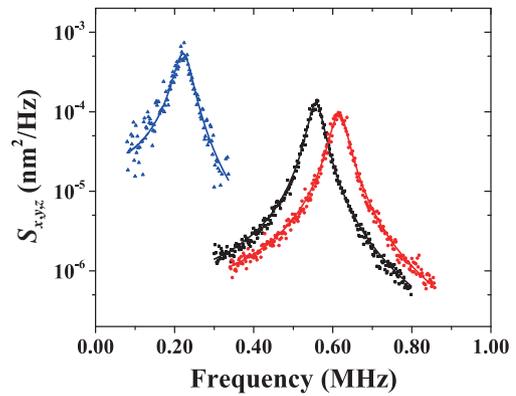

Figure 2 (Color online) The noise spectra @6.8 kPa in the three dimensions with RBW 20 Hz and VBW 100 Hz. Blue triangle for z, dark square for x, red dot for y.
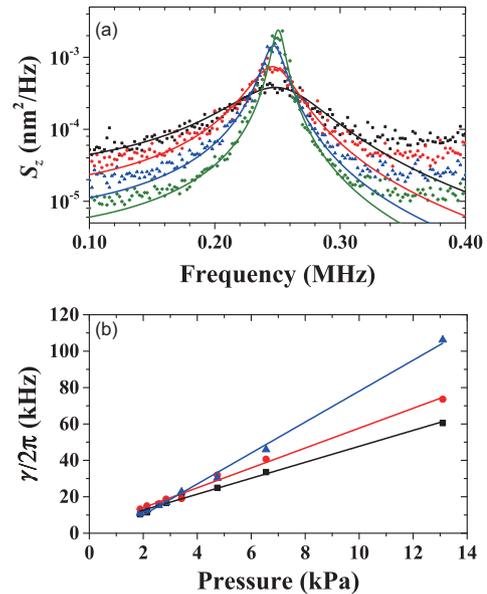

Figure 3 (Color online) (a) Noise spectra in the z direction vs. the air pressure. The black, red, blue, and green traces correspond to $p = 13.1$, 6.55, 3.42, and 1.89 kPa, respectively. (b) Measured damping rate of the x, y, z oscillations vs. the air pressure. Blue triangles stand for z, dark squares for x, red dots for y.
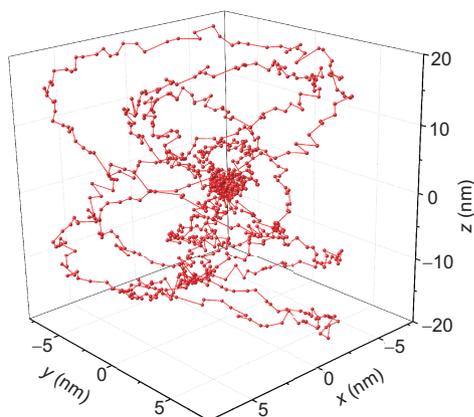
Figure 4 (Color online) The center-of-mass motion trajectory of the levitated particle.

the black, red, blue, and green traces correspond to p =13.1, 6.55, 3.42, and 1.89 kPa, respectively) and Figure 3(b) is the corresponding damping rates in the three dimensions.

The information of the three-dimension position can be recorded simultaneously by a multi-channel oscilloscope. So according to the signals, the motion trajectory of the particle in the space can be plotted. Figure 4 is the spatial motion trajectory with the noise which corresponds to the Brownian motion caused by the air molecules.

In conclusion, we experimentally realized the optical trapping of the nanosphere. The spatial motion trajectory is recovered according to the position information of the three dimensions. The trapping frequency is far from the low frequency range. The high degree squeezed light is easily obtained in the relative high frequency (>100 kHz) at the current experiment [19, 20]. Thus the motion of the trapped nanosphere can be detected with squeezed-state optical field in the future.

1 S. Singh, G. A. Phelps, D. S. Goldbaum, E. M. Wright, and P. Meystre, Phys. Rev. Lett. **105**, 213602 (2010), arXiv: 1005.3568.
2 T. Li, S. Kheifets, and M. G. Raizen, Nat. Phys. **7**, 527 (2011), arXiv: 1101.1283.
3 J. Gieseler, B. Deutsch, R. Quidant, and L. Novotny, Phys. Rev. Lett. **109**, 103603 (2012), arXiv: 1202.6435.
4 J. Gieseler, L. Novotny, and R. Quidant, Nat. Phys. **9**, 806 (2013), arXiv: 1307.4684.
5 O. Romero-Isart, M. L. Juan, R. Quidant, and J. I. Cirac, New J. Phys. **12**, 033015 (2010), arXiv: 0909.1469.
6 F. Ricci, R. A. Rica, M. Spasenović, J. Gieseler, L. Rondin, L. Novotny, and R. Quidant, Nat. Commun. **8**, 15141 (2017), arXiv: 1705.04061.
7 A. A. Geraci, S. B. Papp, and J. Kitching, Phys. Rev. Lett. **105**, 101101 (2010), arXiv: 1006.0261.
8 Z. Yin, T. Li, and M. Feng, Phys. Rev. A **83**, 013816 (2011), arXiv: 1007.0827.
9 J. Millen, T. Deesuwan, P. Barker, and J. Anders, Nat. Nanotech. **9**, 425 (2014), arXiv: 1309.3990.
10 L. P. Neukirch, E. von Haartman, J. M. Rosenholm, and A. Nick Vamivakas, Nat. Photon **9**, 653 (2015).
11 J. Li, I. M. Haghighi, N. Malossi, S. Zippilli, and D. Vitali, New J. Phys. **17**, 103037 (2015), arXiv: 1506.03126.
12 J. Zhang, T. Zhang, and J. Li, Phys. Rev. A **95**, 012141 (2017), arXiv: 1611.09989.
13 A. Bassi, K. Lochan, S. Satin, T. P. Singh, and H. Ulbricht, Rev. Mod. Phys. **85**, 471 (2013), arXiv: 1204.4325.
14 T. Li, S. Kheifets, D. Medellin, and M. G. Raizen, Science **328**, 1673 (2010).
15 P. Z. G. Fonseca, E. B. Aranas, J. Millen, T. S. Monteiro, and P. F. Barker, Phys. Rev. Lett. **117**, 173602 (2016), arXiv: 1511.08482.
16 V. Jain, J. Gieseler, C. Moritz, C. Dellago, R. Quidant, and L. Novotny, Phys. Rev. Lett. **116**, 243601 (2016), arXiv: 1603.03420.
17 L. Rayleigh, Phil. Mag. **47**, 375 (1899).
18 Y. Harada, and T. Asakura, Opt. Commun. **124**, 529 (1996).
19 W. Li, Y. B. Jin, and X. D. Yu, Sci. China-Phys. Mech. Astron. **60**, 050321 (2017).
20 W. Yang, S. Shi, Y. Wang, W. Ma, Y. Zheng, and K. Peng, Opt. Lett. **42**, 4553 (2017).